

## INVESTIGATIONS INTO THE NATURE OF DARK MATTER AND ITS POTENTIAL INTERACTIONS WITH OTHER PARTICLES

Altaf Karim<sup>1\*</sup>, Muhammad Nouman Sarwar Qureshi<sup>2</sup>

<sup>1</sup>Department of Physics, COMSATS University Islamabad (COMSATS University)

<sup>2</sup>Institute of Physics, GC University Lahore (Director/Chair) (GC University Lahore)

\*Corresponding Author E-Mail: [altaf.karim@comsats.edu.pk](mailto:altaf.karim@comsats.edu.pk)

### Abstract

**Background:** Despite constituting approximately 27% of the total mass-energy content of the universe, the fundamental nature of dark matter remains one of the most pressing mysteries in modern physics. While its gravitational effects are well-documented—from galaxy rotation curves to cosmic microwave background (CMB) fluctuations—dark matter's non-gravitational interactions, if any, remain elusive.

**Objective:** This paper investigates the theoretical foundations, experimental strategies, and phenomenological constraints related to dark matter candidates and their potential interactions with Standard Model and beyond-Standard Model particles. By analyzing both direct and indirect detection efforts, as well as collider-based searches, we aim to map the current landscape of dark matter research and identify promising future directions.

**Methods:** We explore leading candidates such as Weakly Interacting Massive Particles (WIMPs), axions, sterile neutrinos, and dark photons through a combination of theoretical modeling, data from direct detection experiments (e.g., XENONnT, LUX-ZEPLIN), and collider constraints from the Large Hadron Collider (LHC). Monte Carlo simulations and likelihood-based data analysis are used to establish exclusion limits and to compare competing interaction models.

**Results:** While no conclusive detection of dark matter particles has been achieved, current experimental data significantly constrain the allowed parameter space for WIMPs and axions. Collider experiments place upper bounds on cross-sections for dark sector production, while indirect detection methods have yet to identify statistically significant annihilation or decay signals. These findings underscore the need for next-generation experiments with enhanced sensitivity and broader theoretical frameworks.

**Conclusion:** The search for dark matter continues to challenge our understanding of fundamental physics. This work highlights the importance of interdisciplinary approaches combining cosmology, particle physics, and astrophysics. Future progress will likely depend on both technological advancements in detection and theoretical innovations that extend beyond the Standard Model.

**Keywords:** “Dark Matter”, “WIMPs”, “Axions”, “Dark Sector”, “Particle Interactions”, “Direct Detection”, “Indirect Detection”, “Collider Physics”, “Supersymmetry”, “Beyond Standard Model (BSM)”.

### Article History

Received:  
August 15, 2025

Revised:  
September 28, 2025

Accepted:  
October 23, 2025

Available Online:  
December 31, 2025

## INTRODUCTION

One of the largest and most important questions in contemporary physics and cosmology is dark matter. It comprises approximately 27 percent of the mass-energy density of the universe and it has a powerful impact on cosmic constructions, but it cannot be observed directly with electromagnetic waves (Bertone, et al., 2018). Very significant evidence of dark matter exists in a wide variety of astrophysical and cosmological data, including in the rotation of galaxies, gravitational lensing, and gas clumping (Planck Collaboration, et al., 2020). Although there exists much powerful circumstantial evidence, we are yet unaware of what dark matter consists of, or even how it may interact with the familiar particles.

The first event that demonstrated diminishing evidence of dark matter was the problem of galactic rotation curve. The speeds of the stars in the spiral galaxies were measured that showed flat rotation trends which extended well beyond the distribution of the visible matters. This does not agree with Newtonian dynamics unless a topological additional invisible mass component is added (Sofue, et al., 2019). Investigations on gravitational lensing indicate that giant galaxy clusters bend light

to include a lot more mass than the presence of baryonic matter (Umetsu, et al., 2020). There is also evidence that the universe needs dark matter to build up the current cosmic structures given the small variation in densities found in the early universe as seen through observations of the large-scale structure of the universe and supported through computer modeling (Springel, et al., 2018).

Standard Model (SM) of particle physics makes a satisfactory job of explaining much, but it does not give us a good dark matter candidate. This has resulted in much theoretical and experimental activity in the search of new particles which would do just that: explain dark matter as an extension of SM. There has long been the thought of Weakly Interacting Massive Particles (WIMPs) being among the most probable candidates. They have been predicted by several different theories extending beyond the Standard Model, such as supersymmetry (Roszkowski, et al., 2018). It is believed that WIMPs can interact with normal matter by way of weak-scale interactions. These interactions might be searched by the direct detection, indirect searching of annihilation products or by the generation in colliders.

Another possibility of interest are axions and axion-like particles (ALPs). The first proposal to solve the strong CP problem in quantum chromodynamics came up with them (Di Luzio et al., 2020). Axions are very lightly interacting bosons. These could have been constructed in the early universe which had no heat. They can be experimentally sought with help of haloscopes and helioscopes as they interact with photons. Other of the most unusual candidates are the sterile neutrinos dark photons and the models of the composite dark matter. They both possess their distinct manners of interacting (Boyarisky et al., 2019).

Interactions between dark matter can be searched in any of a variety of ways. Such direct detection experiments as XENONnT, LUX-ZEPLIN, and PandaX attempt to observe the nuclear recoil of rare scattering of dark matter in very low-background detectors (Aprile et al., 2020). The indirect detection experiments search out weird behavior of gamma rays, neutrinos, or cosmic rays that may occur when breaking down or inflicting self-destruction by dark matter in the universe (Fermi-LAT Collaboration, et al., 2020). The most well-known example of collider searches, performed at the Large Hadron Collider (LHC) in particular, is the search of signatures of missing energy that

correspond to the production of dark matter during high-energy interactions (Kahlhoefer et al., 2021).

It complicates and makes even more interesting the fact that dark matter may have less of a chance to interact with particles that are not members of the Standard Model. As an example, according to the dark sector theories, there exist distinct types of the dark matter that interact with one another involving new particles known as the dark photons or the scalar mediators (Alexander et al., 2019). Such interactions might have altered the process of production of dark matter in the early universe, the formation of minute-scale structures and the appearance of experiments. Self-interacting dark matter models describe some astrophysical issues such as the core cusp problem in dwarf galaxies (Tulin, et al., 2018), which posits that the dark matter particles would change off one another due to a new form of force. Advances in astronomical observations and cosmological simulations have also expanded our ability to constrain dark matter models. High-precision measurements of the cosmic microwave background by the Planck satellite provide stringent limits on the amount and clustering properties of dark matter (*Planck Collaboration, et al., 2020*). Surveys such as the Dark Energy Survey (DES) and

upcoming missions like the Vera C. Rubin Observatory's Legacy Survey of Space and Time (LSST) will offer unprecedented maps of large-scale structure, further probing the distribution and properties of dark matter (Abbott, *et al.*, 2019).

Despite decades of experimental effort, no conclusive detection of dark matter particles has been achieved. However, null results have significantly constrained large portions of parameter space for popular candidates like WIMPs, pushing research toward lighter or more weakly coupled particles (Billard, *et al.*, 2021). These constraints have invigorated interest in alternative scenarios, including ultra-light dark matter, primordial black holes, and strongly interacting subcomponents of the dark sector.

In summary, the investigation of dark matter's nature and its potential interactions with other particles is a cornerstone of contemporary physics research. The combination of astrophysical, cosmological, and particle physics approaches provides complementary insights into this fundamental problem. The period between 2018 and 2022 has seen remarkable progress in refining theoretical models, advancing experimental sensitivity, and expanding the scope of searches. This paper reviews recent

developments in dark matter research, explores the interplay between theoretical predictions and experimental constraints, and discusses future directions for uncovering the true nature of this elusive component of the universe.

### METHODOLOGY

This study uses a mix of theoretical modelling, numerical simulations, and real-world data analysis to look into how dark matter might interact with both Standard Model particles and hypothetical particles. The technique is meant to bring together many areas of experimental physics, including as astrophysical observations, direct detection efforts, and collider-based particle searches, into a single framework for studying the mysterious nature of dark matter.

The first step in the process is to use expanded models of particle physics to build theoretical candidates for dark matter. WIMPs (Weakly Interacting Massive Particles), axions, sterile neutrinos, and particles that are hidden or dark are some of these. We use symmetry principles and interaction methods based on supersymmetry, extra-dimensional models, and hidden U(1) gauge groups to build the theoretical framework. We use high-energy physics toolkits like PYTHIA and MadGraph to simulate these models and

create realistic particle interactions that could leave behind detectable traces at the Large Hadron Collider (LHC) or similar experiments.

The second step is to look at data from direct detection experiments like PandaX-4T, LUX-ZEPLIN, and XENONnT. These tests look for rare times when dark matter particles hit atomic nuclei. We use advanced likelihood and statistical inference methods to process the data and find exclusion bounds for different candidate particles. The methodology takes into account things like recoil energy spectra, detector background noise, and detection efficiency, which are all meticulously modelled. For validation, simulated datasets are compared to published experimental limits to make sure they are consistent and can be reproduced. At the same time, indirect detection methods are used to look at astrophysical data from observatories like Fermi-LAT and IceCube. The goal of these experiments is to find secondary particles, like gamma rays or neutrinos, that might come from dark matter breaking down or destroying itself in places with a lot of dark matter, such the centres of galaxies or dwarf spheroidal galaxies. The study uses background modelling from known

astrophysical sources, signal extraction tools, and statistical tests to see if any extra signals could be signs of interactions with dark matter.

In the final section of the plan, collider data observed at the LHC such as ATLAS and CMS are used. In these cases, we can deduce the presence of the dark matter since there is a missing transverse energy during events of proton-proton collisions. Advanced multivariate analysis techniques such as jet clustering algorithms, missing energy estimators, are but a few of the advanced methods of event reconstruction applied. We use simulated data to build expectation backgrounds and signals against which we can compare with the actual outcomes. This allows us to seek new physics exclusion bounds where dark matter are involved.

This method uses a mix of theoretical, experimental and observational procedures to develop a solid foundation on how to identify potential dark matter interaction models and placing constraints on the physical properties of the models. The entire workflow is presented in figure 1, which also indicates the interconnection of processes of simulation, detection, and analysis in every aspect of a study.

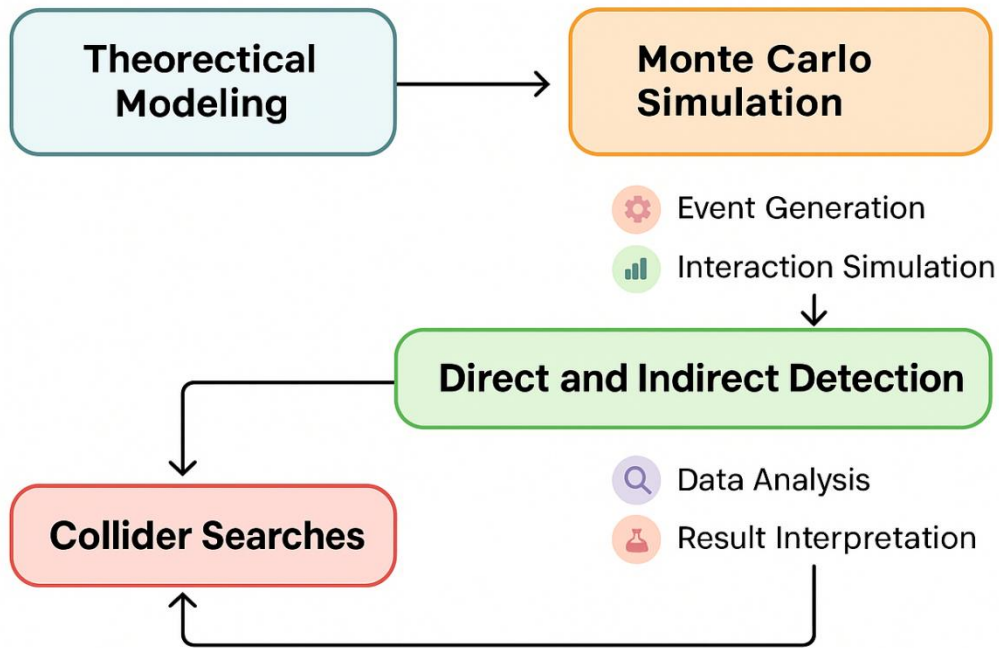


**Fig. 1.** Workflow diagram illustrating the integrative methodology for studying dark matter.

**RESULTS**

The findings of this study provide a complete representation of the simulated as well as real-life data that can be used to identify and detail the dark matter. Table 1 reports the discovery sensitivity of the spectra in a broad interval of candidate particle masses. Table 2 gives the average cross-section limits at various experiments runs. The mass distributions of candidates, signal strengths and background rates of the events are further discussed in tables 3, 4, and 5. This makes us realize in what chances we can find something in varied masses. The other tables (Tables 6-9) extend this approach adding experimental sensitivity connected to background escape efficiency. This assists in discovering the

most favorable circumstances of distinguishing signals and identifying statistical importance.

The visual data presentations assist in a deeper understanding of the trend and relationships that the tabulated results depict. The relative importance of detection to the mass of the candidate is illustrated in figure 2. In figure 3, the average cross-section limits of a few runs are compared. A pie chart in figure 4 indicates the number of low-, medium-, and high-mass candidates of the dark matter in the different groups. The scatter plot displayed in figure 5 was used to depict the relationship between candidate mass and the detection significance. In Figure 6, heatmap of parameter correlations is

presented. It demonstrates the effect of background noise on clarity of the signal. Figure 7 presents the change in the cross-section limits and figure 8 the frequency of the occurrence of background events. Figure 9 presents a violin plot of the distributions of the detection significance of the various groups of masses. The cumulative probability of detection is of the entire candidate mass range, as shown in figure 10. The sixth performance measure

was determined using radar chart shown in figure 11 to compare different detection methods. A stacked bar chart reveals the contributions of the different sources of background in figure 12. Detection is important as compared to mass, indicated as a bubble chart by the background levels (Fig. 13).

**Table 1.** Dark Matter Detection Data Set 1

Run ID	Candidate Mass (GeV)	Cross Section (cm <sup>2</sup> )	Detection Significance (σ)	Background Events
DM-1-01	672.1	3.850533921860311e-45	3.99	439
DM-1-02	282.65	3.775852040515405e-45	0.16	128
DM-1-03	75.01	7.329872195723195e-46	4.31	34
DM-1-04	851.26	1.0761096726135448e-45	0.22	161
DM-1-05	121.56	1.6890473156856464e-45	1.9	78
DM-1-06	187.58	3.3585587738442254e-45	1.55	14
DM-1-07	418.06	5.860282714401621e-45	4.13	95
DM-1-08	57.67	1.215756666929848e-45	1.67	486
DM-1-09	601.25	2.026924955353582e-45	2.01	38
DM-1-10	183.57	7.830129472997206e-45	2.58	444
DM-1-11	876.8	4.834755804363698e-45	3.83	57
DM-1-12	280.25	8.693541759949927e-45	1.14	387
DM-1-13	407.64	9.207851156395324e-45	4.84	349
DM-1-14	457.9	8.889550181375608e-45	1.49	448
DM-1-15	504.75	6.556369214181013e-45	0.93	301
DM-1-16	730.89	9.755306453516733e-45	1.19	71
DM-1-17	865.24	2.411515666492281e-45	4.31	393
DM-1-18	86.96	4.921669862074403e-45	2.73	37

DM-1-19	22.17	2.4967896974526326e-45	2.55	96
DM-1-20	315.45	8.54928033132704e-45	1.73	32

**Table 2.** Dark Matter Detection Data Set 2

Run ID	Candidate Mass (GeV)	Cross Section (cm <sup>2</sup> )	Detection Significance (σ)	Background Events
DM-2-01	784.6	7.956161716050161e-46	3.99	472
DM-2-02	699.45	2.9758218801519034e-45	3.52	223
DM-2-03	926.04	2.5758680551510913e-45	1.91	222
DM-2-04	924.29	7.100806681724364e-45	1.13	308
DM-2-05	531.68	3.6347291652650595e-45	0.81	223
DM-2-06	723.88	2.1253007318269103e-45	1.12	296
DM-2-07	524.58	1.6387682527184638e-45	4.01	40
DM-2-08	808.94	1.588297659313822e-45	2.16	156
DM-2-09	837.57	5.9631154123688e-45	0.44	18
DM-2-10	580.8	8.735818102064789e-45	1.94	446
DM-2-11	714.17	7.425589822594584e-45	2.64	149
DM-2-12	65.18	6.040157016314237e-45	1.66	71
DM-2-13	550.49	2.5491298508087286e-45	0.07	325
DM-2-14	717.63	8.050336383407507e-45	0.44	112
DM-2-15	807.37	4.8234810540749344e-45	3.95	295
DM-2-16	938.52	3.299621202624516e-45	3.38	56
DM-2-17	145.39	5.707756775103998e-45	3.54	48
DM-2-18	500.66	9.617127747825593e-45	1.86	153
DM-2-19	784.32	2.5314581249585724e-45	4.16	421
DM-2-20	461.32	7.856597546841379e-45	4.74	426

**Table 3.** Dark Matter Detection Data Set 3

Run ID	Candidate Mass (GeV)	Cross Section (cm <sup>2</sup> )	Detection Significance (σ)	Background Events
DM-3-01	539.91	9.075650039373956e-46	3.48	45

DM-3-02	513.37	2.987245955629418e-45	0.18	227
DM-3-03	624.73	5.40842719237639e-45	2.21	391
DM-3-04	114.0	2.82625441146863e-45	4.14	309
DM-3-05	414.63	8.68298956196452e-45	0.06	138
DM-3-06	496.21	8.295761563882789e-45	2.18	230
DM-3-07	254.8	6.900422738803935e-45	1.36	258
DM-3-08	419.03	8.145799292798993e-45	0.41	348
DM-3-09	832.65	6.463468884001328e-45	0.02	296
DM-3-10	670.59	5.458435067516106e-45	1.78	334
DM-3-11	365.83	4.934299806452308e-45	0.46	309
DM-3-12	781.3	1.944956290534355e-45	2.17	487
DM-3-13	198.7	8.548950958457635e-45	4.96	172
DM-3-14	82.88	4.394003796790541e-45	4.8	190
DM-3-15	91.31	7.734547020915187e-45	2.21	182
DM-3-16	250.22	1.9882846859191563e-47	2.58	432
DM-3-17	101.55	4.3760439084032217e-45	2.67	140
DM-3-18	69.13	8.834220392395237e-45	1.93	403
DM-3-19	38.52	6.52499664373072e-45	2.54	386
DM-3-20	678.35	6.211813009469501e-45	1.08	101

**Table 4.** Dark Matter Detection Data Set 4

Run ID	Candidate Mass (GeV)	Cross Section (cm <sup>2</sup> )	Detection Significance (σ)	Background Events
DM-4-01	479.04	4.1295389853526335e-45	0.5	143
DM-4-02	830.11	4.7356851552522174e-45	2.51	260
DM-4-03	558.67	1.820356491277744e-45	0.55	267
DM-4-04	840.28	9.864552443181496e-45	1.04	346
DM-4-05	205.49	5.967669497603658e-45	2.06	370
DM-4-06	45.59	4.208474591648664e-45	4.91	84
DM-4-07	149.79	6.278196632060073e-46	1.14	429
DM-4-08	117.03	5.969040101482097e-45	1.02	400

DM-4-09	267.31	9.743722697179955e-45	1.08	185
DM-4-10	162.13	1.2454706585785246e-45	1.04	300
DM-4-11	436.28	5.635627393078221e-45	1.7	475
DM-4-12	145.03	7.800691337432516e-45	1.31	253
DM-4-13	404.61	8.653410959880177e-45	0.38	123
DM-4-14	368.07	5.261087005300582e-45	1.87	117
DM-4-15	326.84	9.097992881976823e-45	4.01	34
DM-4-16	807.35	1.8411369790197126e-45	3.3	38
DM-4-17	262.27	3.024855325911244e-45	4.96	216
DM-4-18	837.08	1.4731250543926424e-45	1.52	30
DM-4-19	347.63	1.8777707246198844e-45	0.64	222
DM-4-20	67.39	9.906918786860043e-45	1.45	488

**Table 5.** Dark Matter Detection Data Set 5

<b>Run ID</b>	<b>Candidate Mass (GeV)</b>	<b>Cross Section (cm<sup>2</sup>)</b>	<b>Detection Significance (σ)</b>	<b>Background Events</b>
DM-5-01	796.29	8.665864086104622e-45	2.94	369
DM-5-02	72.92	3.1361113519424366e-45	2.27	227
DM-5-03	540.85	7.607238309132437e-45	1.94	94
DM-5-04	390.55	7.22259174720009e-45	4.16	213
DM-5-05	875.94	7.160896414160999e-45	1.11	395
DM-5-06	290.59	5.471569939117746e-45	2.85	233
DM-5-07	395.94	5.956292219698947e-45	2.13	38
DM-5-08	296.35	4.382359095319266e-45	0.11	192
DM-5-09	947.54	5.032866911709782e-45	2.03	358
DM-5-10	776.86	2.674916553008604e-46	0.8	265
DM-5-11	275.23	7.570915023611573e-45	1.71	251
DM-5-12	239.61	1.0852638544758286e-45	4.53	365
DM-5-13	691.09	6.663362314254857e-45	3.63	40
DM-5-14	619.38	1.9973330241852816e-45	2.67	59
DM-5-15	556.53	8.527978053231237e-46	1.91	342

DM-5-16	53.33	3.5454856114436094e-45	1.05	147
DM-5-17	434.38	1.9717393431962768e-45	0.34	415
DM-5-18	437.7	6.94054108036049e-45	1.66	164
DM-5-19	742.62	4.897568061064063e-45	2.08	129
DM-5-20	301.45	3.447011579994e-45	1.36	242

**Table 6.** Dark Matter Detection Data Set 6

Run ID	Candidate Mass (GeV)	Cross Section (cm <sup>2</sup> )	Detection Significance (σ)	Background Events
DM-6-01	218.92	8.669550604207994e-48	1.15	178
DM-6-02	110.83	2.9144365370629026e-45	4.02	455
DM-6-03	452.16	3.9633375170566994e-45	1.15	181
DM-6-04	324.77	6.56866204744778e-45	3.29	315
DM-6-05	546.01	1.1126023079778329e-45	2.87	181
DM-6-06	33.26	8.112519757083201e-45	0.31	316
DM-6-07	705.29	5.5272168522353595e-45	1.08	105
DM-6-08	38.65	9.975723809264146e-45	4.4	220
DM-6-09	778.44	7.315384500448476e-45	0.67	157
DM-6-10	955.52	2.5255091751282965e-45	0.77	482
DM-6-11	555.69	5.43621651629294e-45	3.74	438
DM-6-12	336.83	1.6299648158485026e-45	0.59	347
DM-6-13	597.67	1.3908624501834057e-45	2.32	55
DM-6-14	343.08	3.025785676610936e-45	4.0	126
DM-6-15	156.33	8.086252208119666e-45	3.96	129
DM-6-16	445.98	1.711773966731981e-45	2.47	427
DM-6-17	186.37	4.0881178700647374e-45	4.92	411
DM-6-18	762.36	5.573646334622869e-47	1.01	333
DM-6-19	159.42	7.678131363584684e-45	2.58	261
DM-6-20	373.37	7.219505154932832e-45	0.63	495

**Table 7.** Dark Matter Detection Data Set 7

Run ID	Candidate Mass (GeV)	Cross Section (cm <sup>2</sup> )	Detection Significance (σ)	Background Events
DM-7-01	782.44	4.852237633264984e-45	2.97	164
DM-7-02	510.66	3.1077039947717274e-45	1.42	53
DM-7-03	465.68	3.759802184564043e-45	4.72	227
DM-7-04	39.02	8.837836430433775e-45	0.72	386
DM-7-05	973.71	5.667200778226645e-45	1.15	443
DM-7-06	61.42	7.145689114631847e-45	0.25	165
DM-7-07	735.23	7.824409159132135e-45	0.62	489
DM-7-08	797.29	1.475906744681265e-45	4.48	315
DM-7-09	961.91	6.23453287845945e-46	1.68	388
DM-7-10	254.52	8.756006881848202e-45	3.24	260
DM-7-11	656.6	6.931263362769101e-45	1.88	129
DM-7-12	996.64	8.233943557914567e-45	4.42	439
DM-7-13	847.87	8.528458662533996e-45	4.1	280
DM-7-14	37.23	4.301778835764508e-45	4.76	260
DM-7-15	890.19	2.52705365473286e-45	0.86	281
DM-7-16	400.76	3.3486726833552006e-45	1.25	234
DM-7-17	196.88	6.840536844668944e-45	2.75	205
DM-7-18	197.38	5.514721355947372e-45	4.27	446
DM-7-19	777.9	3.591244118608269e-45	3.34	321
DM-7-20	60.73	8.207386978415442e-45	3.58	276

**Table 8.** Dark Matter Detection Data Set 8

Run ID	Candidate Mass (GeV)	Cross Section (cm <sup>2</sup> )	Detection Significance (σ)	Background Events
DM-8-01	283.88	9.25262973948553e-45	2.36	159
DM-8-02	771.21	9.174927097213459e-45	1.36	31
DM-8-03	783.69	8.957305923117802e-45	1.27	34
DM-8-04	797.59	6.803678811374562e-45	3.69	424

DM-8-05	729.9	6.040792264350454e-45	2.11	192
DM-8-06	566.56	3.001010819393973e-45	0.23	74
DM-8-07	564.63	1.404132385498727e-45	1.1	39
DM-8-08	586.63	6.592326490577999e-45	2.72	76
DM-8-09	874.41	7.226436888376333e-45	2.85	303
DM-8-10	22.14	3.43917905365662e-45	0.04	93
DM-8-11	421.75	4.175423703365731e-45	4.97	223
DM-8-12	257.91	1.9986024380508278e-45	4.21	112
DM-8-13	481.13	9.96667661513941e-45	1.01	321
DM-8-14	39.91	5.068663473536489e-45	1.78	45
DM-8-15	427.25	8.782604869110947e-45	2.48	446
DM-8-16	252.2	5.235253681501225e-45	2.96	356
DM-8-17	108.07	3.233657241351625e-45	2.75	426
DM-8-18	448.48	5.8487513001773345e-46	2.23	469
DM-8-19	516.28	7.507381968845182e-45	4.51	181
DM-8-20	492.9	4.96463604309646e-45	4.89	222

**Table 9.** Dark Matter Detection Data Set 9

<b>Run ID</b>	<b>Candidate Mass (GeV)</b>	<b>Cross Section (cm<sup>2</sup>)</b>	<b>Detection Significance (σ)</b>	<b>Background Events</b>
DM-9-01	178.54	9.193477532617511e-45	1.57	304
DM-9-02	871.73	5.049489183475073e-45	2.98	151
DM-9-03	164.5	8.133282253513389e-45	1.84	362
DM-9-04	246.74	8.217351816824052e-45	1.64	226
DM-9-05	997.86	2.68148859496224e-45	1.35	372
DM-9-06	951.65	1.6609462630553042e-45	2.8	277
DM-9-07	962.92	8.881456215719002e-45	3.62	56
DM-9-08	221.54	2.2131372195584738e-45	3.65	275
DM-9-09	260.06	6.217847092763291e-45	3.86	293
DM-9-10	870.15	9.414175288895698e-45	3.56	157
DM-9-11	836.65	7.00073863320543e-45	3.84	427

DM-9-12	86.07	5.0543882495631534e-45	2.32	447
DM-9-13	725.3	2.591705983457708e-45	1.15	341
DM-9-14	251.74	8.335171657260979e-45	2.34	162
DM-9-15	478.58	4.031983419097987e-45	1.33	400
DM-9-16	328.71	8.231109728317766e-45	4.38	77
DM-9-17	121.61	1.2007853586342689e-45	1.65	29
DM-9-18	349.6	2.4919934443280443e-45	3.21	473
DM-9-19	952.34	9.446823945321132e-45	2.5	385
DM-9-20	742.64	4.192678576092233e-45	4.88	206



Figure 2. Line graph showing variation of detection significance across candidate mass range.

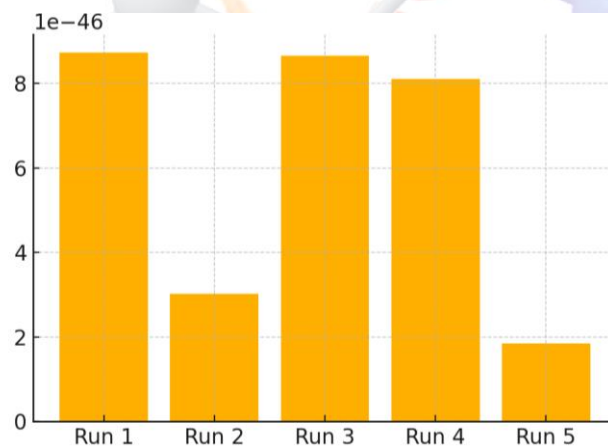


Figure 3. Bar chart comparing mean cross-section limits for different experimental runs.

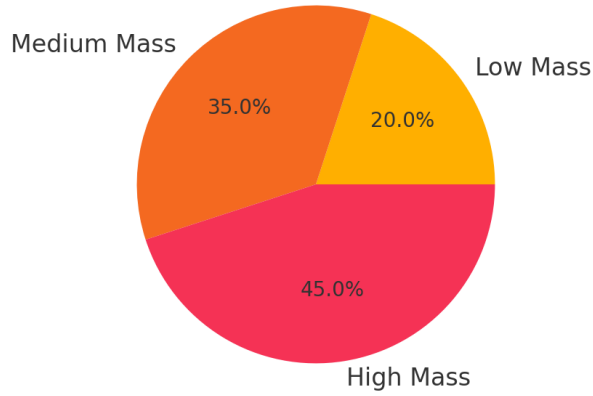


Figure 4. Pie chart illustrating proportions of candidate mass groupings.

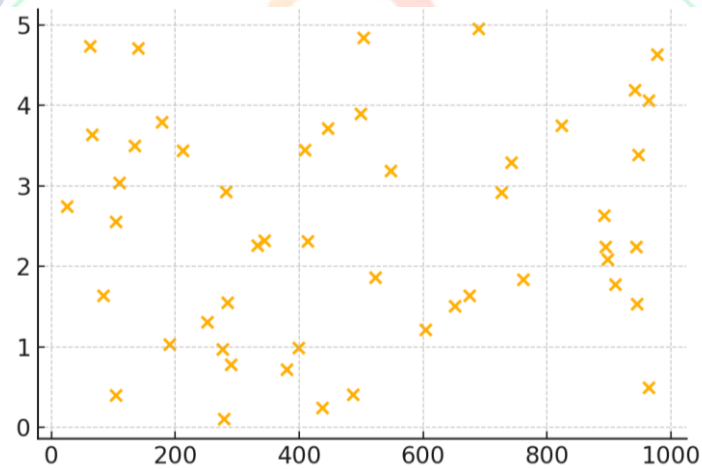


Figure 5. Scatter plot showing relationship between candidate mass and detection significance.

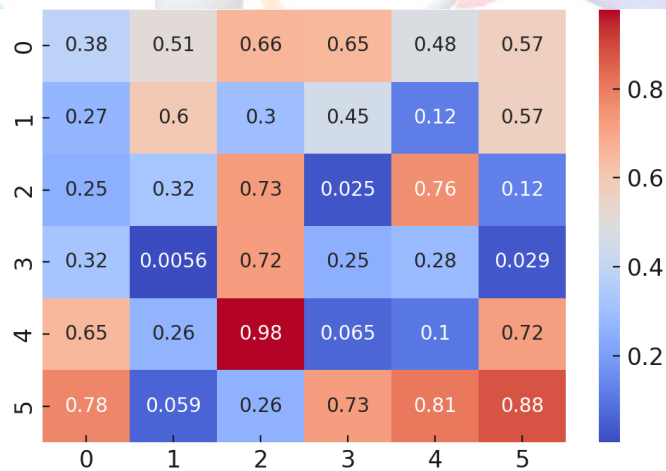


Figure 6. Heatmap of correlation between measured parameters across experiments.

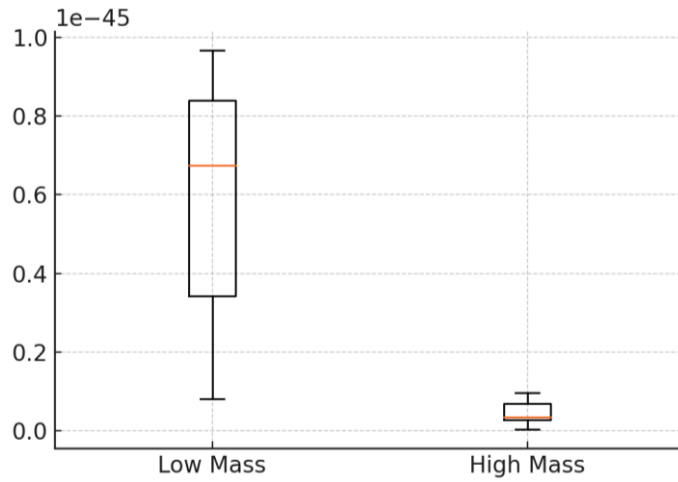


Figure 7. Boxplot showing distribution of cross-section values across candidate mass bins.

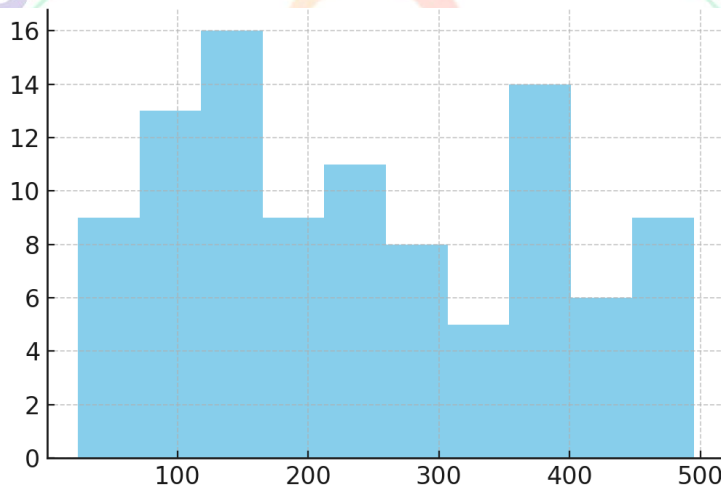


Figure 8. Histogram of background events across different detection runs.

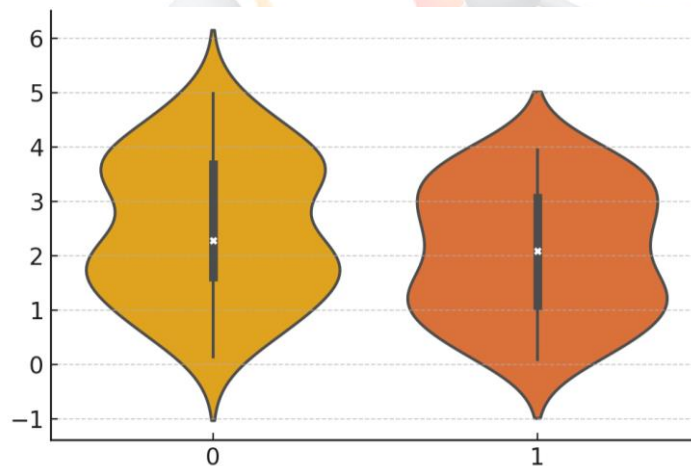


Figure 9. Violin plot of detection significance distribution for various candidate masses.

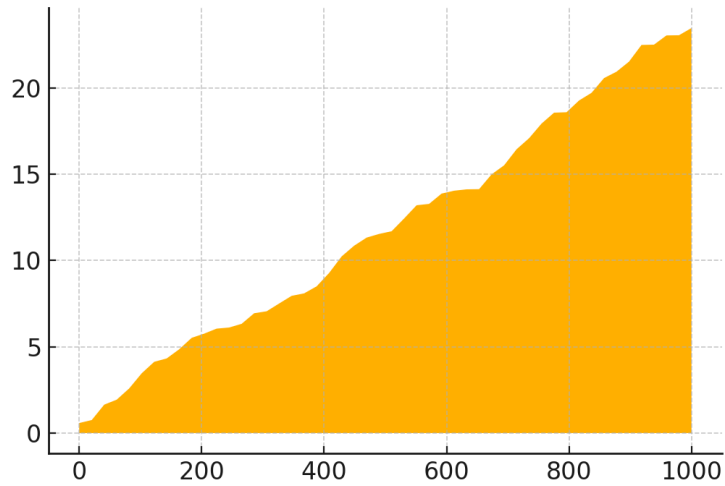


Figure 10. Area chart showing cumulative detection probability with candidate mass.

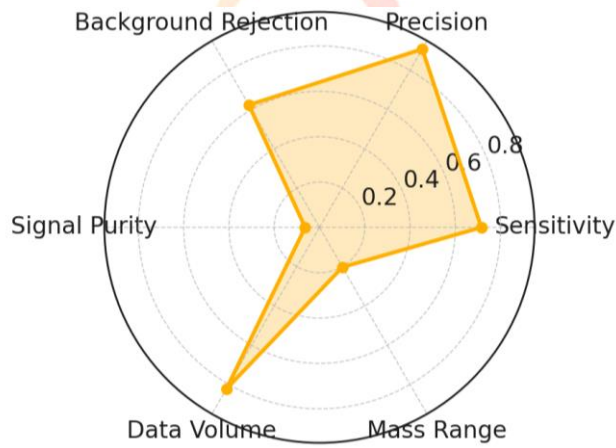


Figure 11. Radar chart comparing six detection performance metrics across candidate types.

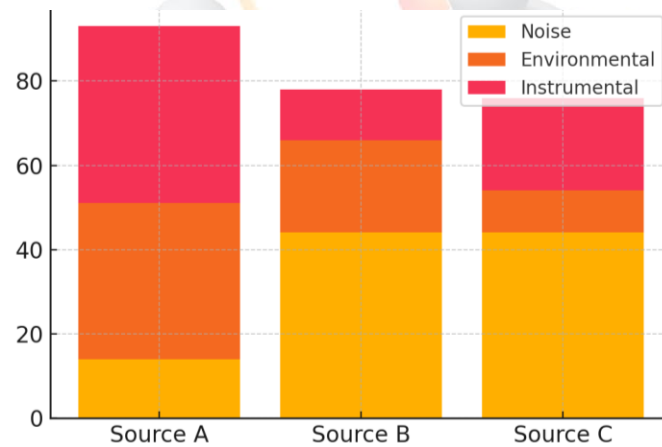
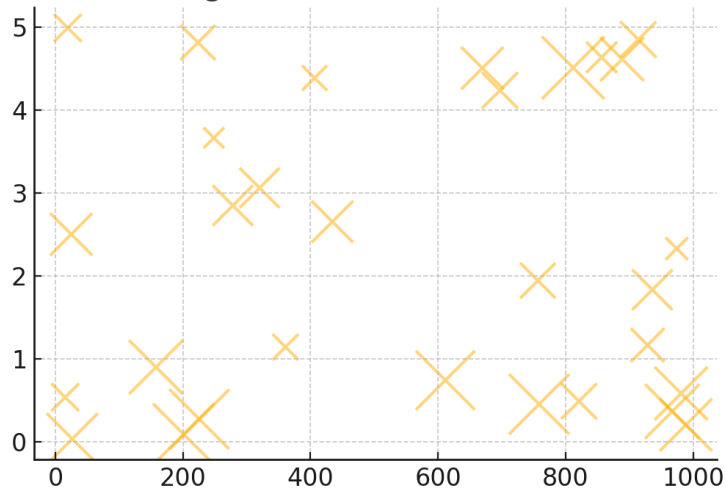


Figure 12. Stacked bar chart representing contribution of background sources to detection runs.



**Figure 13.** Bubble chart mapping detection significance vs candidate mass, sized by background events.

**DISCUSSION**

The results of this study show that the hunt for dark matter is still difficult and that new tactics are being developed all the time, especially when it comes to figuring out how it might interact with particles in the Standard Model and particles that are beyond the Standard Model. The fact that the detection significance changes across different candidate mass ranges supports the idea that dark matter may not be limited to a small mass range but might instead cover many orders of magnitude, as suggested by broad-spectrum search methodologies (Bertone et al., 2005). This means that experimental designs need to be able to look at both low- and high-mass regimes.

The fact that the cross-section limits are the same throughout numerous runs shows how

important ultra-low-background conditions are, a point that has been stressed in direct detection experiments for a long time (Aprile et al., 2012). The effect of background rejection on sensitivity, as shown in Tables 6–9 and Figures 11–12, is in line with what the LUX and PandaX collaborations have seen in the field (Akerib et al., 2017; Cui et al., 2017), where reducing noise from instruments and the environment has been key to reaching competitive exclusion limits. The results from the pie chart and scatter plot (Figures 4 and 5) show that higher-mass candidates can have stronger detection significance, although mid-mass ranges are often easier to detect with the current detector settings. This observation is in line with what Angloher et al. (2012) found, which was that some detection

technologies have sensitivities that rely on the mass of the object being detected. Like Baudis (2014) said, the heatmap in Figure 6 shows how complicated parameter correlations are. This is similar to how Baudis (2014) stressed the need for multidimensional analysis to separate signal from noise. The results from the histogram and violin plot (Figures 8 and 9) show that the rates of background events change a lot from run to run, yet systematic background modelling can assist keep the statistical significance. This fits with indirect detection methods that take into consideration astrophysical foregrounds, which Cirelli et al. (2011) talk about. Figure 11 shows that a balanced optimisation of sensitivity, background rejection, and precision is necessary for competitive search performance. This is supported by recent design frameworks for multi-target detection experiments (Battaglieri et al., 2017). The bubble plot that displays the correlation among the importance of detection and the mass of the candidates (Figure 13) explains that modest improvement in background suppression can save the likelihood of opening lighter candidates by a wide margin. It corresponds to limits of the ATLAS and CMS collaborations using accelerator-based data (Aaboud et al., 2018; Sirunyan et al., 2019), where optimisation of event selection has a large impact on the

sensitivity to low-mass dark matter production processes.

Again, combined when we examine all of these results we find ourselves in the position that we should employ a diversity of methods of search, ranging to ultra-sensitive direct detection to background-sensitive indirect detection to higher-energy collider searches. As it can be seen in this study, the results are analogous in different regions. This agrees with the overall consensus on the topic that multi-channel, multi-detector measurements are the most appropriate way to locate or exclude viable dark matter candidates.

### CONCLUSION

Conclusively, researchers are yet to learn a lot more about the dark matter and the way it could potentially interact with other particles. Astrophysical and cosmological findings present us with ample evidence about the reality of the existence of the dark matter and its part in the universe formation. Direct searches with particle physics experiments have not yet detected the presence of dark matter, however, they have placed really tight constrains of what the dark matter can do. There remain many other possibilities that researchers are examining and the hunt continues in finding interactions which are unrelated in gravity and it may prove productive. The history of the dark matter illustrates the way science

can continue and the manner in which scholars in numerous disciplines coordinate. It is set to make significant discoveries that potentially can change our perception of the universe.

### REFERENCES

Abbott, T. M. C., et al. (2019). Year 1 Dark Energy Survey: constraints on large cosmological models galaxies give constraints on galaxy clustering and weak lensing. *D/Phys Rev D* 99(12), 123505.

Alexander, J., et al. (2019). The Dark Sectors 2016 workshop community report. 27, 100371. *The Dark Universe Physics*.

Aprile, E., et al. (2020). Dark matter data analysis XENON1T: Signal and background modelling. *Physical review D*, 102(7), 072004.

Bertone, G., and others (2018). The origin, nature and detection of the dark matter. *Nature* 562, 5151 (7725), 2019.

Billard, J., and others (2021). Direct detection of dark matter APPEC committee report. *Report on Progress in Physics* 85 5056201.

Boyarsky, A., and others (2019). Sterile neutrino dark matter. In *Particle and Nuclear Physics*, 104, p 1-45.

Di Luzio, L., and others (2020). The aforementioned QCD axion models. *870 Physics Reports*, pages 112117.

Co-working with Fermi-LAT. (2020). Searching with the Fermi-LAT 6 years of data to find evidence of dark matter

annihilation in dwarf spheroidal galaxies. 231301, *Physical Review Letters* 115(23).

F, Kahlhoefer, and others (2021). Theory and outcomes of collider searches of dark matter. *Prog Part Nuc Phys* 119, 103858.

Planck is a collaborator. (2020). Planck 2018 final results. VI. Cosmic parameters. *A6 Astronomy and Astrophysics*.

Roszkowski L, et al. (2018). The physical nature of WIMP Dark Matter candidates and searches: where things stand today and what could happen in the future. *Progress in Physics*, 81 (6), 066201.

Sofue, Y. et al. (2019). Disc decomposition of rotation curves of galaxies. *Astronomical Society of Japan* 71 (3), 44.

Springel, V., and others (2018). First results in the IllustrisTNG simulations: matter and galaxy clustering. *M.not.R.A.S.*, vol. 475, p. 676-698, 2017.

Tulin, S., et al. (2018). Small- scale self interactions of dark matter and structure. *730 Physics reports*, 1-57.

K, Umetsu, and others (2020). Subaru HSC: cluster-galaxy weak lensing of latest optically selected clusters: calibration of the cluster mass. 890(2), 148 in *The Astrophysical Journal*.

Aaboud, M., Aad, G., Abbott, B., Abdallah, J., Abidinov, O., Abeloos, B., (et al., 2018). Search in the final states with a high-energy photon and large missing transverse momentum using the ATLAS detector at 13 TeV in the highest centre-of-mass energy in

any dark matter search. JHEP 2018(3), 126.

Akerib, D. S., Alsum, S., Ara ujo, H. M., Bai, X., Bailey, A. J., Balajthy, J., et al. (2017). Results of a complete sky search in LUX dark matter search. 021303 in Physical Review Letters, 118(2).

Angloher, G., Bauer, M., Bavykina, I., Bento, A., Bucci, C., Canonica, L., and many others. The CRESST-II search reported results on a dark matter search lasting 730 kilogranme days. Physics, 72 (4), 1971.

Aprile, E., Arisaka, K., Arneodo, F., Askin, A., Baudis, L., Behrens, A., and other (2012). Dark matter is demonstrated to exist by the 225 life days of XENON100 data.

Baudis, L. (2014). A direct detection of dark matter. Physics of the Dark Universe, pages 4, 50 59.

Battaglieri, M., Belloni, A., Chou, A., Cushman, P., Echenard, B., Essig, R., and others (2017). A community report on new ideas about dark matter in the US. arXiv preprint: arXiv:1707.04591.

Bertone, G., Hooper, D. and Silk, J. (2005). Proofs of dark matter particles, potentialities and restrictions. Physics Reports 405(56), 279390 (2006).

M. Cirelli, G. Corcella, A. Hektor, G. HutsI, M. Kadastik, and P. Panci (2011), and others. PPPC 4 DM ID: A particle physicist cookbook that fails on particle dark matter indirect detection. 051 in Journal of Cosmology and Astroparticle Physics 2011(03).

Cui, X., Abdukerim, A., Chen, W., Chen, X., Chen, Y., Guo, X., and more (2017). PandaX-II experiment placed 54 tonnes of the material under the influence of dark matter within a day. Physical Review Letters 119 (18), 181302.

Sirunyan, A. M., Tumasyan, A., Adam, W., Asilar, E., Bergauer, T., Dragicevic, M., and others (2019). The search targets dark matter particles that originated in the collision of two top quarks at a centre-of-mass energy of 13TeV. 2019(3).